Presence of Oligomers at Subcritical Actin Concentrations†

Jay Newman,‡ James E. Estes,*,§,∥ Lynn A. Selden,§ and Lewis C. Gershman§,∥

Department of Physics, Union College, Schenectady, New York 12308, Research Service, Veterans Administration Medical Center, Albany, New York 12208, and Department of Physiology, Albany Medical College, Albany, New York 12208

Received May 25, 1984

ABSTRACT: It is generally considered that measurable amounts of actin polymer do not exist at actin concentrations less than the critical actin concentration. However, the theoretical description of actin polymerization proposed by Oosawa and his colleagues implies the presence of oligomers below the critical actin concentration. Using the method of intensity fluctuation spectroscopy, we provide experimental evidence that oligomers do exist at subcritical actin concentrations. A value of $(7.88 \pm 0.11) \times 10^{-7}$ cm^2 s^{-1} was obtained for the infinite dilution translational diffusion coefficient of monomeric actin. After addition of 0.1 mM $MgCl_2$, the diffusion coefficient (D_{20}) measured at a 90° scattering angle for 20 μM actin decreased by 25% within 1–2 h and remained constant for several hours. This decrease in D_{20} could be partially reversed upon addition of low concentrations of $CaCl_2$, indicating that the decrease in D_{20} was not due to denaturation. Using subcritical concentrations of actin labeled with *N*-(1-pyrenyl)iodoacetamide, we determined the time course of oligomer formation to take 80–100 min, which is markedly longer than the time required for exchange of the actin-bound Ca^{2+} for Mg^{2+}. These results demonstrate the presence of oligomers at actin concentrations below the critical actin concentration and suggest that it is Mg-actin that is undergoing oligomerization.

In the late 1950s Oosawa and his colleagues proposed that a critical concentration of monomeric actin must be present in solution before polymer formation could begin (Oosawa et al., 1959). Experimentally, it is now well established that the critical actin concentration (c_c) depends on the solution conditions, e.g., pH, temperature, and ionic strength. Recent work has demonstrated that the species of cation bound to the tightly bound divalent cation site in the monomeric actin structure also plays a major role in determining the c_c (Selden et al., 1983; Gershman et al., 1984). If monomeric actin is present in solutions at a concentration greater than the c_c, polymer formation begins with the aggregation of monomers into nuclei (nucleation step), which then grow into F-actin filaments by the linear addition of monomers onto the ends of nuclei or oligomers (elongation step) (Oosawa & Asakura, 1975; Oosawa, 1983). It is generally accepted that no net formation of polymer is possible below the c_c.

In earlier work in which we studied the activation of the heavy meromyosin ATPase by various polymerization states of actin (Estes & Gershman, 1978), we consistently observed such activation at actin concentrations 1–3 μM below the c_c determined by viscosity. We concluded at that time that "in the region of the critical actin concentration a state of actin exists which appears to be monomeric in viscosity but has the proteolytic digestibility and the ATPase activating ability of F-actin". Offer et al. (1972) reported activation of the myosin subfragment 1 ATPase activity by what they presumed to be G-actin in 5 mM KCl and 0.1 mM $MgCl_2$. Recently, Brenner & Korn (1980, 1981) reported that actin at subcritical concentrations in 0.5 mM $MgCl_2$ will hydrolyze substantial amounts of ATP. However, the solution conditions employed in the studies by both Offer et al. (1972) and Brenner & Korn (1980, 1981) included substantial concentrations of $MgCl_2$, which we now know strongly promotes nucleation and oligomerization (Tobacman & Korn, 1983; Selden et al., 1983). Moreover, Jen et al. (1982) studied the viscoelastic properties of G-actin prepared by the method of Spudich & Watt (1971) with and without gel filtration and observed small aggregates at low ionic strength and 25 °C, particularly in the non-column-purified material. They suggested that some short actin filaments cannot be separated from true G-actin monomers by ultracentrifugation but are removed by gel filtration.

By extending the theoretical work of Oosawa (Oosawa & Asakura, 1975; Oosawa, 1983), we can provide a theoretical basis for the existence of oligomers below the c_c. We have used intensity fluctuation spectroscopy to measure the diffusion coefficient for monomeric actin and have studied the process of oligomer formation below the c_c in the presence of low $MgCl_2$ concentrations by following changes in the average diffusion coefficient. We further confirmed the presence of oligomers below the c_c by determining the time course of oligomerization with monomeric actin labeled with *N*-(1-pyrenyl)iodoacetamide (N-P).[1]

Theoretical Considerations

The helical polymerization theory for actin polymerization was initially proposed by Oosawa & Kasai (1962). The notation and derivation presented here and eq 1–3, 5, and 6 are from the recent review by Oosawa (1983). The theory postulates that an excess free energy (δ) is required for several monomers to form a nucleus, after which polymer growth occurs by the successive addition of monomers, each at free energy ϵ^*, onto the nucleus. At thermodynamic equilibrium, the number concentration of polymers composed of i monomeric units is given by

$$c_i = \sigma K^{-1}(Kc_1)^i \qquad (1)$$

† This investigation was supported by the Veterans Administration and The Research Corporation. A preliminary report of this work has appeared (Newman et al., 1984).

* Address correspondence to this author at the Veterans Administration Medical Center.

‡ Union College.

§ Veterans Administration Medical Center.

∥ Albany Medical College.

[1] Abbreviations: N-P, *N*-(1-pyrenyl)iodoacetamide; EGTA, ethylene glycol bis(β-aminoethyl ether)-*N*,*N*,*N*′,*N*′-tetraacetic acid; tris, tris(hydroxymethyl)aminomethane.

0006-2960/85/0424-1538$01.50/0

where

$$\sigma = \exp(-\delta/kT) \quad (2)$$

$$K = \exp(-\epsilon^*/kT) \quad (3)$$

with c_1 being the number concentration of dispersed monomers, k the Boltzmann constant, and T the absolute temperature. The number concentration of all polymers, c_m, is approximately

$$c_m = \sum_{i=n}^{\infty} c_i \simeq \sigma c_1/(1 - Kc_1) \quad (4)$$

where n is the number of monomeric units in a nucleus. Similarly, the total concentration of monomers incorporated in the polymer fraction, c_h, is approximately

$$c_h = \sum_{i=n}^{\infty} ic_i \simeq \sigma c_1/(1 - Kc_1)^2 \quad (5)$$

The total actin concentration c_0 is given approximately by

$$c_0 = c_1 + c_h \simeq c_1 + \sigma c_1/(1 - Kc_1)^2 \quad (6)$$

At this point in his derivation, Oosawa (1983) indicates that the equilibrium polymer concentration "is negligibly small" until the actin concentration c_0 approaches the critical concentration c_c, defined as $c_c = K^{-1}$. As c_0 exceeds c_c, c_h increases in proportion to the increase in c_0 (above c_c), while the monomer concentration c_1 remains at c_c. He notes that the existence of a critical concentration is due to a small value for σ (a large free energy of nucleation). Oosawa's discussion then continues without further consideration of the character of polymers present when $c_0 < c_c$. It is evident from an inspection of eq 4 and 5 that as long as c_1 is nonzero, c_m and c_h are nonzero, even well below the c_c, and that c_m and c_h are proportional to σ. Thus, a high σ (low free energy of nucleation) is associated with higher values for c_m and c_h at subcritical concentrations.

To demonstrate this more graphically, eq 6 is multiplied through by $K(1 - Kc_1)^2$ and rearranged into a form cubic in the dimensionless variable (Kc_1):

$$(Kc_1)^3 - (2 + Kc_0)(Kc_1)^2 + (1 + 2Kc_0 + \sigma)Kc_1 - Kc_0 = 0 \quad (7)$$

Equation 7 is then easily solved for Kc_1 as a function of σ and the dimensionless variable Kc_0. (This variable is useful in that c_c occurs at $Kc_0 = 1$.) Kc_m and Kc_h may then be calculated by using eq 4 and 5.

Kc_1 and Kc_h for $\sigma = 10^{-5}$ and $\sigma = 10^{-2}$ are graphed in Figure 1, along with "magnified" representations of Kc_m. It is evident that Kc_m is markedly dependent on σ (curve e vs. curve f). Also, when $\sigma = 10^{-5}$, the c_c is sharply defined and the polymer present when $Kc_0 < 1$ can be safely described as "negligible". However, the c_c is less sharply defined when $\sigma = 10^{-2}$ and there is significant polymer present when $Kc_0 < 1$ (hatched area, Figure 1). Curve e indicates Kc_m (×10) for $\sigma = 10^{-2}$; note that even below the c_c, the magnitude of Kc_m is significant in comparison with its magnitude when $Kc_0 > 1$. Thus, when the free energy of nucleation is low, one should expect to observe measurable quantities of polymer at total actin concentrations less than c_c.

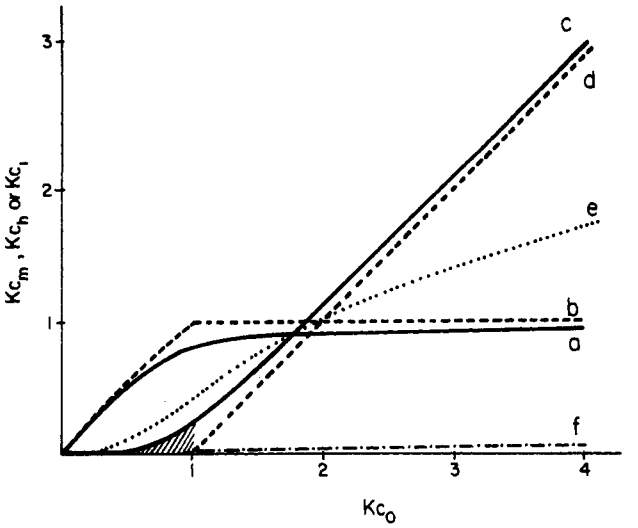

FIGURE 1: Theoretical dependence of Kc_1, Kc_h, and Kc_m on Kc_0 for large and small values of σ, where c_1 = concentration of dispersed monomers, c_h = total concentration of monomer units incorporated into polymer, c_m = number concentrations of all polymers, and c_0 = total actin concentration. Curve a, Kc_1 for $\sigma = 10^{-2}$; curve b, Kc_1 for $\sigma = 10^{-5}$; curve c, Kc_h for $\sigma = 10^{-2}$; curve d, Kc_h for $\sigma = 10^{-5}$; curve e, Kc_m for $\sigma = 10^{-2}$; curve f, Kc_m for $\sigma = 10^{-5}$. For clarity, curves e and f are depicted at 10× their actual value. The σ values were chosen for illustrative purposes only to represent theoretical examples of strong and weak nucleation.

Materials and Methods

All reagents were analytical grade with ATP and EGTA being purchased from Sigma Chemical Co., phalloidin from Boehringer-Mannheim, ^{45}Ca from New England Nuclear, and N-P from Molecular Probes. All solutions were prepared with doubly distilled water.

Actin was extracted from rabbit muscle acetone powder (Szent-Gyorgyi, 1951) and purified by previously published procedures (Estes et al., 1981) with the following modifications: The crude extract was polymerized with 0.1 M KCl and 2 mM $MgCl_2$ (final concentrations). The pellets resulting from centrifugation of the actin after incubation in 0.8 M KCl were homogenized in 0.1 M KCl, 2 mM $MgCl_2$, 0.2 mM ATP, 0.1 mM $CaCl_2$, 2 mM Tris, pH 7.8, and 0.01% NaN_3 and centrifuged again for 2 h at 170000g. After these pellets were homogenized in 1 mM ATP, 0.2 mM $CaCl_2$, 2 mM Tris, pH 7.8, and 0.01% NaN_3, they were dialyzed against 0.2 mM ATP, 0.2 mM $CaCl_2$, 2 mM Tris, pH 7.8, and 0.01% NaN_3 (dialysis solution) for three 12-h periods. The preparation was then sonicated twice for 10 s each, centrifuged for 3 h at 170000g, filtered through a 0.45-μm Millipore filter, and dialyzed further against dialysis solution for two 24-h periods. Finally, the preparation was chromatographed on S-300 Sephacryl with 0.2 mM ATP, 0.02 mM $CaCl_2$, 2 mM Tris, pH 7.8, and 0.01% NaN_3 as the eluent (column buffer). We found that using 0.2 mM $CaCl_2$ where noted instead of 0.02 mM $CaCl_2$ as employed earlier (Estes et al., 1981) tended to result in less aggregated material in the column purification step. The actin prepared by this procedure (Ca-actin) contained 1 mol of tightly bound Ca^{2+}/mol of monomeric protein.

Actin was labeled with N-P by the method of Kouyama & Mihashi (1981) with modifications as reported earlier (Gershman et al., 1984). Phalloidin-stabilized nuclei or oligomers ("seeds") were also prepared as earlier reported (Gershman et al., 1984). Viscosity measurements were accomplished as in Estes et al. (1981), and the measurement of fluorescence intensity changes followed the procedure reported in Gershman et al. (1984). Analysis of the actin-bound divalent cation was performed by using ^{45}Ca-labeled monomeric actin and determining the amount of radioactivity in the actin pellets collected after polymerization of the actin by addition of KCl to 100 mM and equimolar (with actin) phalloidin and ultracentrifugation at 150000g for 3 h following the procedure in Gershman et al. (1984). Atomic absorption measurements of actin-bound Mg^{2+} were also performed on these same pellets by the procedure reported in Gershman et al. (1984). Atomic

absorption measurements were made with a Model 103 Perkin-Elmer atomic absorption spectrophotometer, and radioactivity was measured with a Model 4530 Packard liquid scintillation system.

Polarized intensity fluctuation spectroscopic measurements were performed on actin samples with a previously described apparatus (Newman & Carlson, 1980; Newman et al., 1982). The light source was either the 488- or 514.5-nm beam from an intensity-stabilized Ar^+ laser with a power of 100–200 mW incident on the samples, which were contained in standard 1 cm × 1 cm optical cuvettes. Because of the very low intensity of the scattered light, the apertures in the collection optics were opened so that approximately two coherence areas were viewed by the detector (resulting in normalized signal amplitudes in the intensity autocorrelation function, $g^2(\tau) - 1$, of ~0.55). Measurements were performed at a temperature of 23.0 ± 0.1 °C (data corrected to 20 °C) and typically at several scattering angles in the range of 60–100°. Calibration of the optical system using 0.109-μm polystyrene latex spheres indicated that the same translational diffusion coefficient, within a 1% uncertainty, was obtained at different scattering angles in the range 10–100°.

Actin samples were clarified for the light scattering experiments by filtration through 80 nm pore ultrafilters (Nucleopore) at a rate of ~0.2 mL/min, into optical cuvettes that had been previously cleaned inside a special acetone refluxing apparatus (Newman et al., 1982). The typical scattered intensity at a 90° scattering angle was 8 photocounts s^{-1} mW^{-1} $(\mu M \text{ actin})^{-1}$ with our collection optics, so that count rates were in the range of 5–60 kHz. Prescaled normalized intensity autocorrelation functions were analyzed by the method of cumulants (Koppel, 1972). Typically, 5–10 experiments, each of ~5-min duration, were performed, and the individually normalized experimental data (using the independently measured background levels) were averaged prior to analysis. The average decay rate of the intensity autocorrelation function obtained from a cumulant analysis, $\bar{\Gamma}$, is simply related to the z-average translational diffusion coefficient, D, by $\bar{\Gamma} = 2Dq^2$, where $q = (4\pi/\lambda) \sin(\theta/2)$, λ is the wavelength of the light in the solvent medium, and θ is the scattering angle. All error limits represent standard deviations from the mean value.

Results

Monomeric Actin. Dynamic light scattering experiments were performed on actin samples in column buffer to measure the mutual translational diffusion coefficient of monomeric actin. We found no difference between the diffusion coefficients obtained from actin samples with or without the fluorescent probe N-P as long as the actin was run through a Sephacryl S-300 column as a final purification step. However, if this final step was omitted (even if column-purified actin was labeled with N-P), we found that the diffusion coefficient obtained from labeled actin preparations was significantly (~25%) lower than that of unlabeled preparations. An example of the quality of the raw data for a normalized prescaled intensity autocorrelation function, $g^2(\tau) - 1$, for actin in column buffer is presented in Figure 2 (open circles). The data are well described by a single-exponential decay, indicating a relatively homogeneous population of scatterers.

Figure 3 shows the dependence of the average diffusion coefficient corrected to 20 °C, D_{20}, on $\sin^2(\theta/2)$ over a range of scattering angles from 40 to 100° for a solution of 20 μM actin in column buffer (open circles). A monodisperse solution of noninteracting Rayleigh scatterers would have a diffusion coefficient that is independent of scattering angle. Above a 50° scattering angle our measured D_{20} values are independent of angle as would be expected; however, there is a decrease in the apparent diffusion coefficient at lower angles, indicating the presence of some larger material in our preparations. This could be due to some residual "dust" that is not detected in

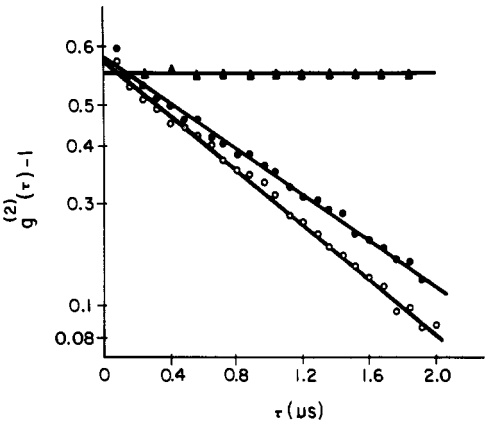

FIGURE 2: Normalized prescaled intensity autocorrelation function, $g^2(\tau) - 1$, of a 20 μM actin sample measured at a scattering angle of 90° and a temperature of 25 °C. The open circles (○) represent the average data from three experiments in column buffer. The filled circles (●) represent the average of three experiments performed approximately 1 h after the addition of 0.1 mM $MgCl_2$. The triangles (▲) are a similar average after the addition of 1 mM $MgCl_2$. A cumulant analysis yields D_{20}(no $MgCl_2$) = (8.10 ± 0.17) × 10^{-7} cm^2 s^{-1} and D_{20}(0.1 mM $MgCl_2$) = (6.57 ± 0.26) × 10^{-7} cm^2 s^{-1}, a 19% lower value. Data recorded with larger channel times, τ, result in D_{20}(1 mM $MgCl_2$) = (0.15 ± 0.02) × 10^{-7} cm^2 s^{-1}, a factor of 54 lower. The cumulant quality of fit parameter was 0.03 for the case of no $MgCl_2$, indicating a good fit to a single relaxation time. For 0.1 and 1 mM $MgCl_2$, the parameter was 0.12 and 0.5, respectively, indicating increasing polydispersity. The data in the first channel were systematically high due to spurious pulses from the phototube, and these data were omitted from computer fits.

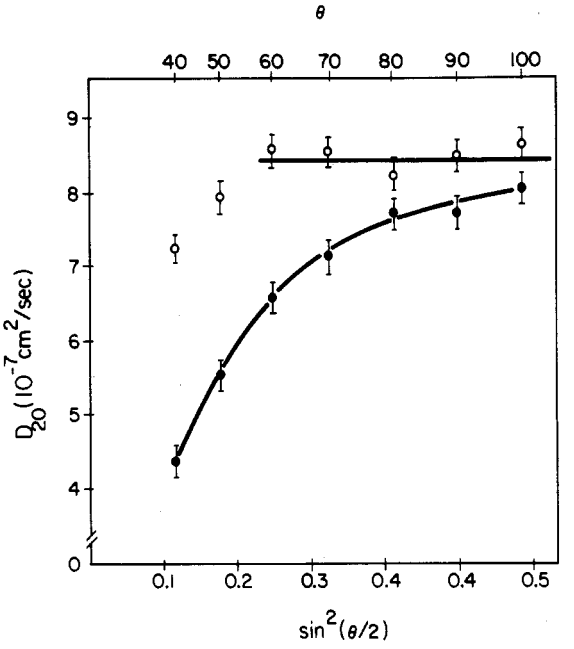

FIGURE 3: Dependence of the apparent diffusion coefficient on $\sin^2(\theta/2)$ for a 20 μM actin sample in column buffer (○) and with added 0.1 mM $MgCl_2$ (●). The decrease in the apparent D_{20}(no $MgCl_2$) at lower scattering angles indicates the presence of a small amount of nonmonomeric actin in our original preparations. However, on addition of 0.1 mM $MgCl_2$, a pronounced decrease in D_{20} occurs at decreasing scattering angles. The data shown are for one sample; measurements on other samples gave qualitatively similar results although there was considerable variability in the magnitude of the decrease of D_{20}(0.1 mM $MgCl_2$) relative to D_{20}(no $MgCl_2$). The error bars represent one standard deviation of multiple determinations.

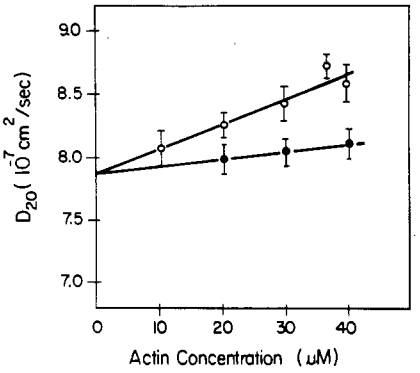

FIGURE 4: Concentration dependence of D_{20} for actin in column buffer (○) or in column buffer containing 0.2 mM $CaCl_2$ (●). By linear extrapolation, the infinite dilution translational diffusion coefficient is $D^0_{20} = (7.88 \pm 0.11) \times 10^{-7}$ cm^2 s^{-1} in column buffer and $(7.86 \pm 0.10) \times 10^{-7}$ cm^2 s^{-1} in column buffer containing 0.2 mM $CaCl_2$. The concentration virial is $(1.9 \pm 0.4) \times 10^{-9}$ cm^2 s^{-1} μM^{-1} in column buffer and $(0.6 \pm 0.3) \times 10^{-9}$ cm^2 s^{-1} μM^{-1} in column buffer containing 0.2 mM $CaCl_2$.

our polystyrene sphere calibration experiments or to some nonmonomeric actin species present in small amounts.

At each concentration of actin studied, a weighted average of D_{20} values at scattering angles above 50° was obtained. Figure 4 (open circles) shows the concentration dependence of D_{20} values obtained from samples from five different preparations of actin. Extrapolation to infinite dilution yields $D^0_{20} = (7.88 \pm 0.11) \times 10^{-7}$ cm^2 s^{-1} and a concentration virial coefficient of $(1.9 \pm 0.4) \times 10^{-9}$ cm^2 s^{-1} μM^{-1}. For purposes of comparison with previous work by others, we also measured D_{20} on one preparation of actin that had been prepared by passage through a Sephacryl S-300 column in our column buffer but with 0.2 mM $CaCl_2$ present (filled circles, Figure 4). Measurements at three concentrations of this actin resulted in a value of $D^0_{20} = (7.86 \pm 0.10) \times 10^{-7}$ cm^2 s^{-1} and a concentration virial coefficient of $(0.6 \pm 0.3) \times 10^{-9}$ cm^2 s^{-1} μM^{-1} under these conditions.

Choice of Solvent Conditions and Critical Actin Concentration Determination. In order to study the early stages of actin polymerization, we examined solutions of actin under conditions where no polymer is considered to form (below the c_c). Since light scattering studies of actin require moderate actin concentrations (~20 μM), very small amounts of added $MgCl_2$, approximately equivalent to the ATP concentration (0.2 mM), will lead to some polymer formation, although at a very slow rate. We chose to study actin solutions in column buffer (containing 0.02 mM $CaCl_2$) to which 0.1 mM $MgCl_2$ has been added because such conditions favor the formation of modest concentrations of Mg-containing actin (Mg-actin) while limiting the total divalent cation concentration to only 0.12 mM. We used two independent measurements to establish that the actin concentrations used under these conditions were below the c_c. First, the specific viscosities of 20 μM actin samples in column buffer or 20 μM actin samples incubated for up to 24 h in column buffer with 0.1 mM $MgCl_2$ added were indistinguishable and have a value about 0.0035. This value is quite representative of published monomeric actin results (Drabikowski & Gergely, 1962; Rich & Estes, 1976). Second, an assay was used to measure the c_c, which is similar to the "initial polymerization slope" method described previously (Selden et al. 1983). Aliquots of phalloidin-stabilized seeds were added to samples of N-P actin that had been equilibrated with column buffer containing 0.1 mM $MgCl_2$ for 1 h, and the fluorescence intensity was monitored for 4 h. In this assay, if no change in fluorescence intensity is observed,

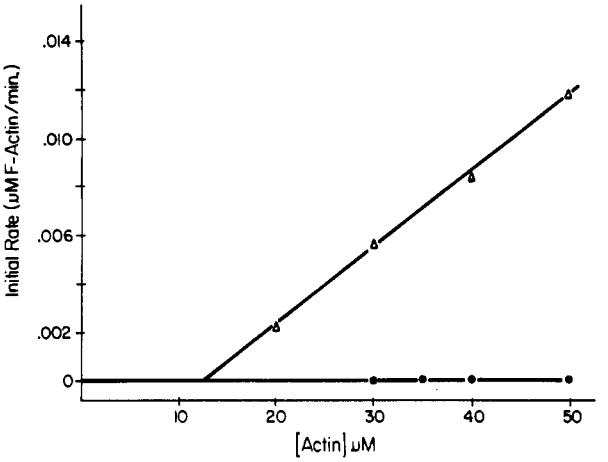

FIGURE 5: Determination of critical actin concentration. Various concentrations of N-P-labeled actin in column buffer were incubated with 0.1 mM $MgCl_2$ (final concentration) for 1 h prior to adding 0.062 M phalloidin-stabilized seeds (final concentration) and monitoring fluorescence intensity for an additional 4 h. (●) N-P-labeled actin in column buffer plus 0.1 mM $MgCl_2$; (△) 100% Mg-actin prepared as in Gershman et al. (1984) with 0.1 mM $MgCl_2$ (final concentration) present.

Table I: Average Diffusion Coefficient of Actin in the Presence and Absence of 0.1 mM $MgCl_2$[a]

total actin concn (μM)	D_{20} (10^{-7} cm^2 s^{-1}) control	D_{20} (10^{-7} cm^2 s^{-1}) with 0.1 mM $MgCl_2$	Mg-actin concn[c] (μM) with 0.1 mM $MgCl_2$
7	7.64 ± 0.05	6.4 ± 0.6	2.3
14	8.03 ± 0.15	5.8 ± 0.6	5.4
20	8.24 ± 0.12	6.2 ± 0.7	7.0
20[b]	7.9 ± 0.4[b]	6.7 ± 0.6[b]	2.0[b]

[a] Conditions: 0.02 mM $CaCl_2$, 0.2 mM ATP, 2 mM Tris, pH 7.8, and 0.01% NaN_3; 90° scattering angle. The error values are estimates of one standard deviation. [b] Samples contain 0.2 mM $CaCl_2$ (final concentration). [c] See Materials and Methods for the procedure used to measure actin-bound Mg^{2+}.

the sample contains actin at a concentration lower than the c_c. In the experiment described in Figure 5 (circles), no change in fluorescence intensity could be detected 4 h after seeds were added to various concentrations of actin in column buffer and 0.1 mM $MgCl_2$. Apparently, the c_c under these conditions was above 50 μM. It should be noted, however, that while no evidence of polymer could be detected after 5 h of incubation at all the actin concentrations examined, after continued incubation of these samples for 24 h, small amounts of polymer could be detected by a small increase in the fluorescence intensity in the higher actin concentration samples (35–50 μM).

We considered that actin equilibrated with 0.1 mM $MgCl_2$ may contain a mixture of Ca-actin and Mg-actin, and we have shown that the c_c for these two species of actin are markedly different (Selden et al., 1983). The results of measuring the actin-bound cation by ^{45}Ca and by atomic absorption (Gershman et al., 1984) are shown in Table I and demonstrate that this is indeed the case. For example, about 7 μM of the 20 μM actin sample is Mg-actin and the remaining portion of the sample is Ca-actin. This 7 μM Mg-actin fraction of the sample is below the c_c for 100% Mg-actin, which has a value of 12.5 μM as shown in Figure 5 (triangles).

Experiments in the Presence of Mg. A typical example of a normalized intensity correlation function obtained from an actin sample in column buffer that had been incubated with 0.1 mM $MgCl_2$ for ~1 h is shown in Figure 2 (filled circles).

For the data shown, a 19% decrease in D_{20} was observed after incubation, together with a 4-fold increase in the cumulant quality of fit parameter. Thus, addition of 0.1 mM $MgCl_2$ resulted in an increase in the effective hydrodynamic size and a decrease in the homogeneity of the sample population. Also shown, for comparison, in Figure 2 (triangles) are similar data obtained after the addition of 1 mM $MgCl_2$ to form fully polymerized actin. In this case, the D_{20} value decreased by a factor of more than 50 and the polydispersity index increased to ~0.5.

Figure 3 shows the dependence of D_{20} on $\sin^2(\theta/2)$ for 20 μM actin with 0.1 mM $MgCl_2$ added (filled circles). Note the lower values at all scattering angles and the steeper decrease in D_{20} with decreasing scattering angle as compared to samples in column buffer only. The values of D_{20} measured at 90° at three different concentrations of actin in the presence and absence of 0.1 mM $MgCl_2$ are compared in Table I. These results represent averages for at least three different preparations of actin. At each concentration a significant decrease in D_{20} was observed after 1–2-h incubation with 0.1 mM $MgCl_2$. We have observed such a decrease in many other preparations of actin under slightly different experimental conditions as well. The relatively large uncertainties in the D_{20} values in the presence of $MgCl_2$ are due to differences from preparation to preparation. Because of these uncertainties and the limited actin concentration range experimentally accessible, no concentration dependence of D_{20} in the presence of 0.1 mM $MgCl_2$ is observed.

In order to determine if the decrease in D_{20} in the presence of 0.1 mM $MgCl_2$ is due to irreversible aggregation, we performed the following experiment with three different preparations of 20 μM actin in 0.2 mM ATP, 0.02 mM $CaCl_2$, 2 mM Tris, pH 7.8, and 0.01% NaN_3 at a 90° scattering angle. First, the diffusion coefficient of actin samples in column buffer was measured and a value of $(8.20 \pm 0.2) \times 10^{-7}$ cm^2 s^{-1} obtained. These samples were then incubated with 0.1 mM $MgCl_2$ for 1–2 h, and the average diffusion coefficient was determined to be $(6.3 \pm 0.4) \times 10^{-7}$ cm^2 s^{-1}. Then an additional 0.1 mM $CaCl_2$ was added to the samples, and after a 1–2-h further incubation, the average diffusion coefficient was again determined and found to have increased to $(7.5 \pm 0.2) \times 10^{-7}$ cm^2 s^{-1}. Clearly a major portion of the decrease in D_{20} after 0.1 mM $MgCl_2$ addition can be reversed by the addition of 0.1 mM $CaCl_2$.

Time Course of Oligomer Formation. If oligomers are formed in a monomeric actin solution during incubation with 0.1 mM $MgCl_2$, then the addition of more salt to aliquots of the solution, lowering the c_c to just below the actin concentration, should allow the detection of enhanced polymerization. Neglecting the effects of de novo nucleation due to the added salt, the rate of polymerization in such an experiment would be approximately proportional to the concentration of oligomers initially present. $CaCl_2$ was chosen as the added salt to avoid further formation of Mg-actin, and 0.3 mM was found to be the concentration of $CaCl_2$ to enhance the addition of monomeric actin onto the ends of existing oligomers while minimizing additional nucleation. The results of such an experiment are described by the solid curve (circles) in Figure 6. To aliquots of N-P-labeled actin with 0.1 mM $MgCl_2$ added at $t = 0$ was added 0.3 mM $CaCl_2$ (final concentration) at time t, and the initial rate of fluorescence intensity increase was measured. The inset shows typical measurements of the initial fluorescence intensity increase upon the addition of 0.3 mM $CaCl_2$. Note that, for the curve for $t = 110$ min (inset), there is very little curvature of the fluorescence intensity increase with time after addition of 0.3 mM $CaCl_2$; this is consistent with the occurrence of marked nucleation of the actin incubated in 0.1 mM $MgCl_2$ prior to the addition of $CaCl_2$. When the rates, calculated from the initial slopes of curves such as in the inset, are plotted against the time, t, after addition of 0.1 mM $MgCl_2$ (Figure 6, solid curve, circles), it is evident that an increase in the rate of add on occurs up to about 110 min, after which a slight decrease in the add-on rate is observed. The results of five separate experiments showed the length of time for maximum oligomer formation to vary between 60 and 100 min.

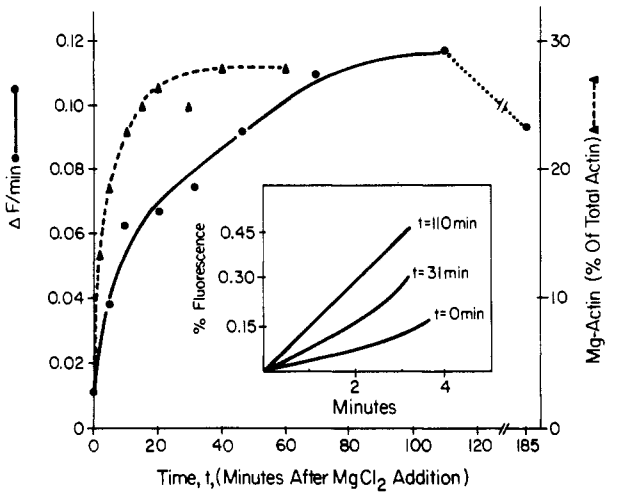

FIGURE 6: Time course for formation of oligomers and exchange of actin-bound divalent cation. Conditions (all concentrations final): 20 μM N-P-labeled actin, 0.2 mM ATP, 0.02 mM $CaCl_2$, 2 mM Tris, pH 7.8, 0.01% NaN_3, and 0.1 mM $MgCl_2$ added at $t = 0$ and $T = 25$ °C. Enhancement of polymerization assay (●): At various times after the addition of 0.1 mM $MgCl_2$ to a solution of N-P-labeled actin, $CaCl_2$ was added to a final concentration of 0.3 mM to aliquots of the solution and the initial rate of polymerization determined from the rate of fluorescence intensity increase. These rates were then plotted against the length of time, t, after addition of $MgCl_2$. In some experiments (not shown here), 0.2–0.25 mM $CaCl_2$ (final concentration) was added to the aliquots with qualitatively similar results as shown with added 0.3 mM $CaCl_2$. Actin-bound Mg^{2+} content (▲): The amount of Mg^{2+} bound to actin (expressed is the percent of total actin) was determined as described in Gershman et al. (1984) in aliquots of monomeric actin that had been polymerized as described in the text.

To demonstrate that this time course does not simply reflect the formation of Mg-actin, the time course of exchange of the actin-bound Ca^{2+} for Mg^{2+} was measured under the same conditions that oligomerization was studied. Monomeric actin was labeled with ^{45}Ca and incubated with 0.1 mM $MgCl_2$. At various times aliquots were removed and the cation exchange was stopped by the addition of 0.1 M KCl, equimolar phalloidin, and 0.062 μM phalloidin-stabilized seeds (all final concentrations). This procedure stopped the cation-exchange reaction by polymerizing both Mg-actin and Ca-actin within 2 min. After sedimentation of the actin polymers in each sample, analyses of each pellet for Mg^{2+} content by atomic absorption and for Ca^{2+} by ^{45}Ca measurements were performed. The dashed curve (triangles) in Figure 6 shows the increase in Mg^{2+} content up to a plateau, whose magnitude is determined by the conditions of the incubation. The exchange reaction is essentially complete within 20 min after addition of 0.1 mM $MgCl_2$, while oligomer formation requires 80–100 min. This implies that oligomer formation is a process distinct from the divalent cation exchange that precedes it.

Discussion

It is generally accepted that there is no net polymer present

in actin solutions at concentrations below the c_c, and there have been no reports of the experimental detection of polymer under such conditions. However, the theoretical description of actin polymerization proposed by Oosawa and his colleagues implies the existence of oligomers at actin concentrations below the c_c. It is not surprising that these oligomers have not been detected; in studies on actin under typical strongly polymerizing conditions, the c_c is small and the oligomer concentration at subcritical actin concentrations is probably exceedingly small. Furthermore, methods commonly used to detect actin polymer, such as viscosity and light scattering, are relatively insensitive and are less sensitive to small polymers (oligomers) than to large polymers. We considered that the technique of intensity fluctuation spectroscopy might offer increased sensitivity in the detection of oligomers and initially based our study on this technique. Subsequently, we have been able to support these results with studies of the time course of oligomer formation using an independent method. Recent studies (Selden et al., 1983) have brought to light the significance of the tightly bound divalent cation to actin polymerization. In view of this, the choice of Mg^{2+} as the major divalent cation for oligomerization experiments was fortuitous since Mg^{2+}-actin nucleates much more readily than Ca^{2+}-actin, and this characteristic probably correlates with a lower free energy for nucleation (high σ, cf. Theoretical Considerations).

There have been four previous values reported for the translational diffusion coefficient of monomeric actin. Mihashi (1964) measured a value of 5.28×10^{-7} cm^2 s^{-1} using synthetic boundary cell techniques. Lanni et al. (1981) reported values in the range $(4.9–6.1) \times 10^{-7}$ cm^2 s^{-1}. Recently, Lanni & Ware (1984) have revised this result to a value of 7.15×10^{-7} cm^2 s^{-1}, and Tait & Frieden (1982) obtained a value of 5.7×10^{-7} cm^2 s^{-1}, both results from fluorescence photobleaching recovery experiments that measure the tracer diffusion coefficient. Montague et al. (1983) published a value of 8.13×10^{-7} cm^2 s^{-1} obtained by dynamic light scattering. The results of this study are in agreement with those of Montague et al., who have discussed the discrepancies in the earlier work of Mihashi and of Lanni et al. Lanni & Ware (1984) discuss the expected difference between the tracer and mutual diffusion coefficients for actin at low ionic strength, and their work appears to be in concurrence with our findings. We have found that labeling column-purified actin with N-P leads to a diffusion coefficient of 6×10^{-7} cm^2 s^{-1}, while a subsequent further column purification of the N-P-labeled actin yields values identical with those of unlabeled actin ($\sim 8 \times 10^{-7}$ cm^2 s^{-1}). This points out a potential problem in studies of labeled actin, which might relate to the lower values for the diffusion coefficient obtained by fluorescence techniques.

The concentration dependence of D_{20} that we have measured agrees with the dynamic light scattering study of Montague et al. (1983) for the same solvent conditions (0.2 mM $CaCl_2$). At 0.02 mM $CaCl_2$, the condition for most of our data, the concentration dependence is more than 3 times as large, indicating a substantial ionic strength dependent interaction, although the infinite dilution values of D_{20} in both solvents agree.

Our studies indicate a substantial decrease in the average translational diffusion coefficient of actin after a short incubation with 0.1 mM $MgCl_2$, under conditions at which the actin concentration is well below the c_c. Mozo-Villarias and Ware have made similar observations in preliminary experiments using fluorescence photobleaching recovery methods (personal communication). The experiments that demonstrated the partial reversibility of the decrease in D_{20} are significant in that they rule out irreversible aggregation upon the addition of 0.1 mM $MgCl_2$ as an explanation for the observed decrease. A decrease in the average diffusion coefficient might also arise from a conformational change in the monomeric actin in the presence of $MgCl_2$ leading to an increased effective hydrodynamic size. In fact, Frieden (1982) has proposed a Mg-induced conformational change in monomeric actin. However, we consider it highly unlikely that such a conformational change could be responsible for the 25% decrease in the average translational diffusion coefficient observed in this work.

We, therefore, consider that the changes in the average diffusion coefficient below the c_c are due to a small amount of reversible actin oligomer formed in the presence of low Mg^{2+} concentrations. The degree of oligomerization is small for the following reasons: (1) the raw intensity autocorrelation function data fit single-exponential decays fairly well at scattering angles above 50°, with an average cumulant polydispersity parameter ~ 0.10 (see Figure 1), (2) the greatest net decrease in D_{20} with 0.1 mM $MgCl_2$ added is only about 25%, and (3) the angular dependence of D_{20} is fairly weak compared to that expected for mixtures of monomer and polymer. A computer experiment was performed in which synthetic autocorrelation function data with Gaussian random noise were generated to represent various mixtures, and the data were fit by using the same analysis as for the experimental data. The experiment verified that mixtures of monomer and small amounts of short oligomers would produce an essentially single-exponential autocorrelation function. The fluorescence assays also clearly indicate that the oligomer population is small because of (1) the lack of measurable fluorescence intensity increase upon incubation with 0.1 mM $MgCl_2$ and (2) the small initial rates of polymerization in our fluorescence assays (Figure 6).

The column-purified monomeric actin employed in this study initially contained 1 mol of bound Ca^{2+}/mol of protein. Incubation of this actin with 0.1 mM $MgCl_2$ resulted in exchange of about 30% of the actin-bound Ca^{2+} for Mg^{2+} in 10–20 min. This partial replacement of bound Ca^{2+} by Mg^{2+} occurs before the oligomerization reaction, as assayed by the experiment shown in Figure 6, reaches a maximum. These data are consistent with the hypothesis that monomeric Mg-actin in the actin mixture is the nucleating actin species. The partial reversibility of oligomer formation can therefore be attributed to the partial reconversion of the Mg-actin formed to Ca-actin in the presence of added $CaCl_2$.

The time course of the oligomer formation experiment (Figure 6) demonstrates the development of stable concentrations of functional oligomers within 60–100 min. The fluorescence assay used is sensitive to the number of ends present in the solution; we show relative increases in the number of ends by showing increased add-on of monomers onto these ends, but we can make no estimate of the actual number of oligomers present. In future experiments, it will be of interest to use such an assay to analyze the time course of oligomer formation and relative number of ends with varying monomer concentrations. However, such experiments would be simplified by working with only one actin species (Mg-actin or Ca-actin) present. Preliminary experiments using 100% Mg-actin have indicated that Mg-actin is the species that oligomerizes under these conditions, while 100% Ca-actin does not. In addition, we have observed that Mg-actin polymer solutions contain more ends than Ca-actin polymer solutions at equilibrium under similar conditions. This would be expected if, as we propose here, Mg-actin has a lower free energy

for nucleation, consistent with the theoretical prediction that the number of polymers at equilibrium is determined by the excess free energy of nucleation (Oosawa, 1983).

In summary, the decrease in D_{20} on treatment of actin with 0.1 mM $MgCl_2$ represents the physical aggregation of monomeric units. The observation that this decrease in D_{20} is in large part reversible suggests that this aggregation is not associated with denaturation. The fluorescence intensity experiments (Figure 6) demonstrate the presence of functional nuclei in actin solutions resulting from incubation with 0.1 mM $MgCl_2$. We thus conclude that functional small polymers (oligomers) of actin do exist at actin concentrations lower than the critical actin concentration.

Registry No. Mg, 7439-95-4.

References

Brenner, S., & Korn, E. D. (1980) *J. Biol. Chem. 255*, 841-844.

Brenner, S., & Korn, E. D. (1981) *J. Biol. Chem. 256*, 8663-8670.

Drabikowski, W., & Gergely, J. (1962) *J. Biol. Chem. 237*, 3412-3417.

Estes, J. E., & Gershman, L. C. (1978) *Biochemistry 17*, 2495-2499.

Estes, J. E., Selden, L. A., & Gershman, L. C. (1981) *Biochemistry 20*, 708-712.

Frieden, C. (1982) *J. Biol. Chem. 257*, 2882-2886.

Gershman, L. C., Newman, J., Selden, L. A., & Estes, J. E. (1984) *Biochemistry 23*, 2199-2203.

Jen, C. J., McIntyre, L. V., & Bryan, J. (1982) *Arch. Biochem. Biophys. 216*, 126-132.

Koppel, D. (1972) *J. Chem. Phys. 57*, 4814-4820.

Kouyama, T., & Mihashi, K. (1981) *Eur. J. Biochem. 114*, 35-38.

Lanni, F., & Ware, B. R. (1984) *Biophys. J. 46*, 97-110.

Lanni, F., Taylor, D. L., & Ware, B. R. (1981) *Biophys. J. 35*, 351-364.

Mihashi, K. (1964) *Arch. Biochem. Biophys. 107*, 441-448.

Montague, C., Rhee, K. W., & Carlson, F. D. (1983) *J. Muscle Res. Cell Motil. 4*, 95-101.

Newman, J., & Carlson, F. D. (1980) *Biophys. J. 29*, 37-48.

Newman, J., Day, L. A., Dalack, G. W., & Eden, D. (1982) *Biochemistry 21*, 3352-3358.

Newman, J., Selden, L. A. Gershman, L. C., & Estes, J. E. (1984) *Biophys. J. 45*, 107a.

Offer, G., Baker, H., & Baker, L. (1972) *J. Mol. Biol. 66*, 435-444.

Oosawa, F. (1983) in *Muscle and Non-Muscle Motility* (Stracher, A., Ed.) Vol. 1, pp 151-216, Academic Press, New York.

Oosawa, F., & Kasai, M. (1962) *J. Mol. Biol. 4*, 10-21.

Oosawa, F., & Asakura, S. (1975) *Thermodynamics of the Polymerization of Protein*, Academic Press, New York.

Oosawa, F., Asakura, S., Hoffa, K., Imai, N., & Ooi, T. (1959) *J. Polym. Sci. 37*, 323-336.

Rich, S. A., & Estes, J. E. (1976) *J. Mol. Biol. 104*, 777-792.

Selden, L. A., Estes, J. E., & Gershman, L. C. (1983) *Biochem. Biophys. Res. Commun. 116*, 478-485.

Spudich, J., & Watt, S. (1971) *J. Biol. Chem. 246*, 4866-4871.

Szent-Gyorgyi, A. (1951) *Chemistry of Muscular Contraction*, 2nd ed., Academic Press, New York.

Tait, J. F., & Frieden, C. (1982) *Biochemistry 21*, 3666-3674.

Tobacman, L. S., & Korn, E. D. (1983) *J. Biol. Chem. 258*, 3207-3214.

Actin Oligomers below the Critical Concentration Detected by Fluorescence Photobleaching Recovery†

Angel Mozo-Villarias and Bennie R. Ware*

Department of Chemistry, Syracuse University, Syracuse, New York 13210

Received August 3, 1984

ABSTRACT: Measurement of the diffusion coefficient of G-actin using fluorescence photobleaching recovery reveals that a hydrodynamically larger species is formed in Mg^{2+}-containing buffers but not in Ca^{2+}-containing buffers. In buffer A (2 mM Tris-HCl, 0.2 mM $CaCl_2$, 0.2 mM ATP, and 0.5 mM 2-mercaptoethanol, pH 8.0) and other Ca^{2+}-containing buffers, the data indicate a single species with a diffusion coefficient of (7.98 ± 0.17) × 10^{-7} cm^2/s. In Mg^{2+}-containing buffers the average diffusion coefficient was (5.52 ± 0.06) × 10^{-7} cm^2/s, and there was evidence of more than one component. The distinction between these buffer systems was reversible by dialysis. The conjecture that the putative oligomeric species may be active in promoting actin assembly was confirmed in two independent experiments. Assembly of actin in the presence of these species produced shorter filaments, as would be expected if they act to increase the number of nucleation sites. In addition, trace quantities of these species added to buffer A actin had the ability to accelerate the kinetics of actin assembly. It is concluded that G-actin below the critical concentration forms oligomeric species in the presence of 50-200 μM Mg^{2+} and that these species either are assembly nuclei or at least are more readily converted to assembly nuclei than is monomeric actin.

The capacity of actin for reversible self-assembly is believed to be an indispensable element of its role in cytoplasmic motility (Pollard & Weihing, 1974; Taylor & Condeelis, 1979; Stossel et al., 1982; Korn, 1982). Extensive studies of the kinetics of actin assembly in vitro have led to an established model in which, for any given set of solution conditions, there is a critical concentration of actin that remains unassembled

† This work was supported by Grant PCM-8306006 from the National Science Foundation.

0006-2960/85/0424-1544$01.50/0